Förster Resonance Energy Transfer Across Interpolymer Complexes of poly(acrylic acid) and poly(acrylamide)

Thomas Swift,[ab*] Natalie Paul,[†b] Linda Swanson,[b] Maria Katsikogianni,[b] and Stephen Rimmer[ab*]

0. Abstract

Interpolymer complexes of homopolymer macromolecules are often described as 'laddered' or 'ribbon' type structures. The proposition of the existence of these ladder structures seems to us not reasonable and here we examine this hypothesis. To address this we have used polymers enabled for Förster Energy Transfer (FRET). Chromophores bound to a macromolecular backbone can transfer energy across short distances via FRET. The close binding of poly(acrylamide) and poly(acrylic acid) interpolymer complex formation at low pH forms a structure compact enough for significant energy transfer to occur between different chains containing naphthalene and anthracene labels. In the context of the proposition that ladder polymers can form it was surprising that the distance between labels on the same polymer back-bone was equivalent regardless of whether the polymer was complexed or not. The data indicated that the bicomponent structure may be more compact than previously supposed: I.e. the complexes are not ladders composed of extended chains. This evidence suggests formation not of ordered 'ladder' systems but colloidal 'co-globules'.

1. Introduction

Many aspects of biological systems are determined by interactions of macromolecules that give rise to protein conformational changes[1-2]. It is well known that cooperative interactions in aqueous media of certain synthetic macromolecules can lead to interpolymer complexation[3-7]. This is an important phenomenon in a number of areas of emerging materials science[1]. The complexation is driven either by van der Waals forces to form stereocomplexes[8], polyelectrolyte bindings between polyacids[9], coordination complexes[10] or hydrogen bonding[11-12]. All of these have been investigated over recent years and careful polymer design can lead to new composite materials[8, 13] and new applications as sensors[14-15] or delivery vehicles[11, 16]. There are a variety of methods for detecting interpolymer complexes (IPC) including viscometry, conductivity measurements, NMR spectroscopy and fluorescence[9, 17-19]. Pyrene, which forms excimers as the local pyrene concentration increases, has also been added as a probe to study segmental motion of partially hydrolysed poly(acrylamide) (i.e. PAA-*co*-PAM)[19]. Using these techniques it was proposed that a decrease in excimer formation in the complex indicated the formation of rigid conformations in the complex and extended conformations. However, the same authors also suggested that measurements of intrinsic viscosity showed that complexes had "compact polymer structures"[19-20] and Bain and Liu also showed that the complex formation between PAA and poly(dimethyl acrylamide) gave reductions in intrinsic viscosities as the coils contracted[21].

Other fluorescence techniques can also be used to convey information about the solubility, conformation and structure of dissolved macromolecules[15, 22-25] and we were interested to further probe the nature of chains in these potentially technologically important interpolymer complexes. Both Napthalene and Anthracene are fluorescent units that are useful in studies of large polymeric systems[26-29]. Probing of macromolecules via fluorescence can be used in a variety of ways. These include: the dissolution of a soluble dye into a polymer solution[30]; chemical attachment of a probe directly into the polymer backbone[31] or as a grafted subunit[32]. Acenaphthylene (ACE) is derivative of naphthalene, that when copolymerized into a soluble polymer backbone is linked by two bonds On the other hand 9-anthryl methyl methacrylate (AMMA) is copolymerized to attach an anthracene unit pendant to the main chain backbone (Fig. 1) by an ester linkage. It has been shown that both units report differing information about polymer solution behavior[33].

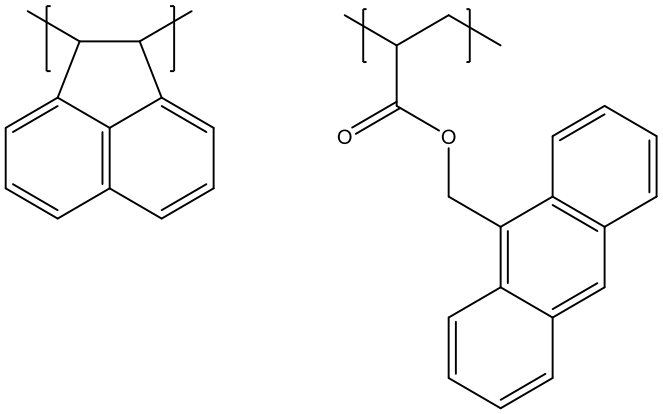

Figure 1. Structures of direct reporting chromophore acenaphthylene (ACE) and pendant subunit 9-anthryl methyl methacrylate (AMMA) copolymerised along polymer backbone.

Förster Resonance Energy Transfer (FRET) uses electronic non-radiative exchanges between 'donor' and 'acceptor' labels to predict molecular scale distances. Multiple studies have shown that transfer efficiency begins to decrease sharply at separations in excess of 30 Angstroms[34] although in fully optimized systems transfer is still possible up to 120 Angstroms[35]. FRET enabled polymers have been considered for some years as potential biosensors (i.e. for oligonucleotides, proteins, inhibitors, enzymes, metal ions) but it is interesting to note that most of these systems use conjugated polymers[36-44]. Whilst conjugated polymers offer excellent light harvesting possibilities they exhibit limited solubility and thus these polymers are only suited to certain applications. Alternatively, in non-conjugated polymers, with pendant chromophores located along the polymer chain[45], or chain ends[1], FRET occurs intramolecularly. For this reason this technique has been used to study the conformation of stimulus responsive polymers[15, 23-24, 46], the formation of supramolecular assemblies[47] or to measure the diffusion across surfaces[25, 48], as the dimensions of the polymer change in response to external stimuli[49]. To achieve this two fluorescent chromophores (ACE and AMMA) have been attached to a single polymer backbone. The communication between these species is dependent on their proximity, on the 1 to 10 nm length scale[28-29]. In FRET measurements one of the chromophores is excited (considered the donor excited state) but then the energy is transmitted non-radiatively to the acceptor chromophore, which then emits via radiative decay. This process can be summarised via the resonant energy transfer process; $D^*+A \rightarrow D+A^*$. As the donor and the acceptor must be in close proximity the effect is reduced by the increased separation of chromophores as the chain volume is increased (Fig. 2). Polymers containing a single chromophore do not undergo FRET processes but other factors can affect their decay, therefore these need to be studied to give suitable reference states.

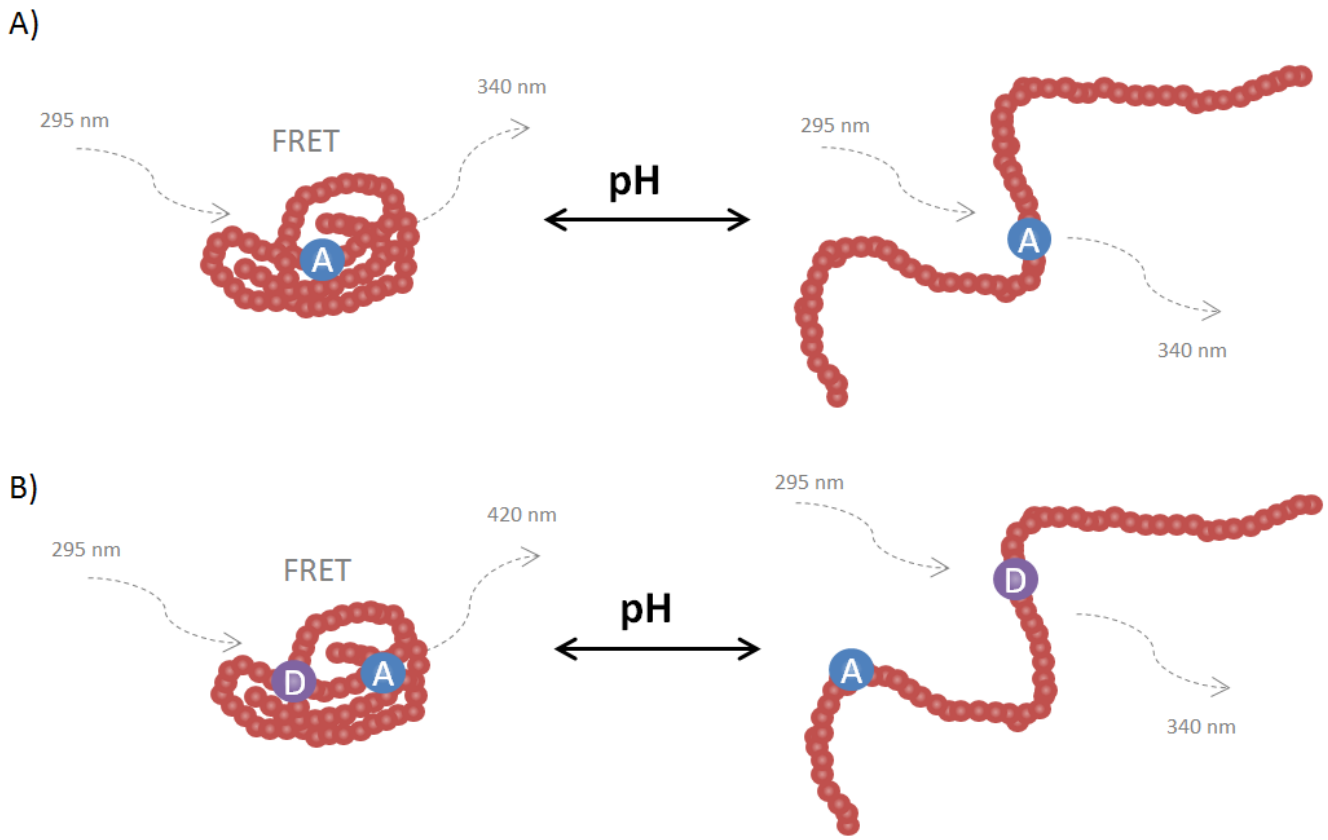

Figure 2. Models showing the coil-to-globule transition of pH responsive polymers containing chromophores. A) Single chromophore system used as control polymer. B) Dual label system containing both donor (D) and acceptor (A) moieties of FRET process. The degree of label separation matches observed changes in polymer hydrodynamic radii.

Attachment of chromophores onto small conjugating oligomeric systems has been carried out before[16, 36, 44]. These studies typically used low molecular weight oligomers or polymers with fluorescent chain ends to tag the end of intercalating dyes[44]. Previous studies have shown these systems can studied using FRET changes across a state change (for example micelle formation[16, 50]) but relatively few studies have examined single-molecule conformation reorganisation or dual molecule IPC formation.

Poly (acrylamide) (PAM) is a commonly used synthetic polymer with a range of applications in materials processing[14] and biotechnology[51-52]. It forms strong IPCs with a range of materials, including poly(acrylic acid) (PAA). In the literature this is often modelled as a 'laddered' or 'zipper' system between two polymer chains. In this work we were interested in the nature of these complexes. In order to do this we employed the two experiments. In the first experiment ACE and AMMA were both copolymerized in small quantities with PAA. This produced a dual labelled polymer in which the FRET process was used to probe the interactions and distances between PAA segments. In the second experiment ACE and AMMA were attached to both polymers separately. This experiment gave information on interaction and complex formation between segments of PAA and PAM. In our previous work and application of this area we have used PAA containing an ACE label to form a highly sensitive anisotropic polarized detection system[15] for detection of ppm level concentrations of interpolymer complexation in fresh water[14].

The generally accepted model describing these systems involves a "zipper" effect in which the two polymer components exist separately then acrylamide and carboxylic acid groups align to form a ladder type structure. However, Deng et al recently used light scattering techniques to show that the individual chains aggregate also in the one component solutions. They interpreted these results by modifying the "zipper" to propose that the complexes evolve within the aggregates that are present in the single component solutions[53].

In this work we have used FRET to further investigate the IPC formed from PAA and PAM. The data showed that polymers are not extended in the complex form and this supports the hypothesis that the complexes are globular entwined structures that could be derived from the process described by Deng[53].

2. Experimental

2.1 Sample Preparation

Materials

All materials were used as supplied and sourced from Sigma-Aldrich unless otherwise stated. Fluorescence label ACE was purified via column chromatography before use.

Synthesis of AMMA

Synthesis of AMMA was performed following a modification of previously published methods[33]. 9-anthracenemethanol (20 g) and triethylamine (40 ml) were added to tetrahydrofuran (400 ml) and dried under nitrogen at 0 °C. Methacryloyl chloride (28 ml) was added dropwise over a period of one hour and stirred for 5 hours over which time the mixture was allowed to warm to room temperature yielding an orange solution and a solid. Distilled water and then diethyl ether were added to extract the organic product from the mixture. The lower aqueous phase was removed, then the ether extract was filtered and washed with deionized water, 0.5 M HCl solution, saturated $NaHCO_3$ solution and then dried over anhydrous sodium sulfate (BDH) for 16 hours at room temperature. The ether was evaporated using a rotary evaporator at room temperature. The product was recrystallized from spectroscopic grade methanol and purified via column chromatography with silica gel. The recrystallized monomer was dried in a vacuum oven at room temperature for several days. The product was a yellow crystalline solid, stored at -10°C. It was identified as the desired product by its melting point (85.3 °C) and its ^{1}H NMR spectrum in $CDCL_3$ (Bruker 400 MHz, δ 1.99 (s CH_3) δ 5.51 (s CH_2) δ 6.05 (s H) δ 6.20 (s H) δ 7.5 (m, Ar) δ 8.32 (m Ar)).

Polymer Synthesis

Polymers were synthesized by adding distilled monomers [acrylic acid (3.0 g, 0.04 moles) / acrylamide (3.0 g, 0.042 moles)] and 4,4'-azobis(isobutyronitrile) (AIBN)) (varying by ratio) in dioxane. Chromophores (ACE / AMMA) were added at varying molar ratio. Samples were thoroughly degassed via three freeze-pump-thaw cycles. Once oxygen had been removed from the system the ampoules were flame sealed and heated to 60 °C in a water bath for three days. Afterwards the precipitated polymer was filtered, dissolved in deionized water and added to rapidly stirring butanol to purify. After repeated purification steps it was left in a vacuum oven until dry. Poly(acrylamide) ^{1}H NMR in D_2O (δ 2.31 (m CH) δ 1.99 (m CH_2) δ 1.6 (m CH_3)). Poly(acrylic acid) ^{1}H NMR in D_20 (δ 2.35 (m CH) m (δ 1.75 CH_2)). Monomer ratios to the polymerization feed are shown in Table 1, full polymer characterisation details and experimental methods are given in the electronic supporting information.

Table 1. Relative Monomer Feed (Molar Ratio) of Polymerisation Reaction

Polymer	AA	AIBN	ACE	AMMA
PAA	100	0.87	-	-
P(AA-co-ACE)	100	0.88	0.52	-
P(AA-co-AMMA)	100	0.73	-	0.38
P(AA-co-ACE-co-AMMA)	100	0.39	0.20	0.44
PAM	100	0.85	-	-
P(AM-co-ACE)	100	0.86	0.56	-
P(AM-co-AMMA)	100	0.94	-	0.35

2.2 Sample Analysis

Size Exclusion Chromatography

Polymer molar mass distributions and moments were calculated using size exclusion chromatography. Molar mass moments were calculated using methylated (via trisdiazomethane) PAA polymers[27] analysed in a tetrahydrofuran mobile phase (passed through a 0.45 μm

pore filter) via 3 x PLgel 10 μm mixed-B LS columns (flow 1 ml ml^{-1}). Label distributions across molar mass were confirmed with an aqueous mobile phase system (flow 1 ml ml^{-1}), with a dual RI and UV detector to give both polymer and label concentrations.

DOSY NMR

Samples were dissolved in D_2O (1 mg ml^{-1}) and analyzed on a Bruker Avance 400 spectrometer, operating at 400 MHz to provide both static ^1H NMR, ^{13}C and ^1H DOSY diffusion constants in m2 s^{-1}. Polymer hydrodynamic radii (R_H) and intrinsic viscosity [η] were calculated utilising methods previously outlined[54].

Particle Size Measurements

Particle size measurements were carried out on a Malvern Zetasizer Nanoseries Nano-ZS. Dilute solutions of polymer (1 mg ml^{-1} of each component) were measured in 1 cm path length quartz cuvettes and measured at 25 °C. Atomic Force Microscopy (AFM) experiments were carried out using an Asylum Research MFP-3D (Santa Barbara, CA) and AC160TS Olympus silicon cantilever probes with a tip radius (Rtip) of 15 nm, a half cone angle of α = 36° and a spring constant of approximately 0.3 N m^{-1}. AFM imaging was carried out using intermittent contact (AC) mode at ambient temperature (22 °C) and humidity (34%). Following laser alignment, calibration of the detector sensitivity and the cantilever spring constant (k ~ 0.32 N m^{-1}) was made using the thermal method. Dilute samples (< 0.1 mg ml^{-1} concentration) were air dried overnight on glass microscope slides. The Igor Pro software was used for the real time control, the data acquisition, as well as for the offline analysis and the data manipulation. Height data from various scan sizes, ranging from 10x10 μm^2 to 0.3 x 0.3 μm^2, were processed using flattening, and the height distribution or the height profile were computed using the Igor Pro software over the scan size or along a cross line section.

Fluorescence Analysis

UV/vis absorbance measurements were carried out in solution (2 mL, < 1 mg ml^{-1} concentration), scanned between 350 – 800 nm, performed in wavelength mode standardized using a user baseline configuration. Steady state spectra of dilute solutions were observed. Both excitation measurements (also known as PLE measurements) and emission measurements were recorded on a Fluoromax-4 Spectrofluorometer (HORIBA Scientific) with an excitation/emission slit width of 1 nm. All solutions were recorded in 10 mm path length quartz cuvettes in ultrapure water.

Static energy transfer (E_{ST}) was obtained from PLE spectra following donor excitation using the equation

$$E_{ST} = \frac{Relative\ Intensity\ of\ Acceptor\ Peak}{Relative\ Intensity\ of\ Donor\ Peak} \quad \text{Eq. 1}$$

where the intensity of the acceptor (AMMA) peak was taken at 420 nm and the donor (ACE) 333 nm.

Fluorescence time resolved lifetime measurements were recorded using an Edinburgh Instruments 199 Fluorescence Spectrometer at an excitation wavelength of 295 nm and an emission wavelength of 340 nm. Measurements were made across 512 channels representing a 200 nanosecond time period. The profile of the laser beam was monitored using a silica prompt to scatter light at the excitation wavelength. All solutions were examined in quartz cuvettes with a path length of 10 mm and then the emitted light was passed through a polarizer that excluded light other than the desired emission wavelength. The excited state lifetime (τ_f) was calculated from the fluorescence decay I(t), where t represents the time, I_o (the initial fluorescence intensity) and A (the instrument offset, from the background noise of the experiment).

$$I(t) = A + B_1 exp\frac{-t}{t_{f1}} + B_2 exp\frac{-t}{t_{f2}} \quad \text{Eq. 2}$$

An alternative (dynamic, or time correlated) method of demonstrating energy transfer using the fluorescence lifetime of the donor species ($E_{D\tau}$) was carried out using Equation 3 where τ_D is the lifetime of the unquenched donor and τ_{ET} is the lifetime of the quenched donor[23].

Between them $E_{D\tau}$ and E_{ST} describe two separate components of fluorescence decay of an excited state (see supporting information). However $E_{D\tau}$ is potentially more useful as it is directly related to the average separation distance (r) between D and A.

$$E_{D\tau} = \frac{{R_0}^6}{{R_0}^6 + r^6} \quad \text{Eq. 3}$$

Here r represents the separation between chromophores, where R_o is the distance where energy transfer is 50%, the critical (Förster) distance. As R_0 for these labels is well known[55] calculation of label separation distances is possible.

3. Results and Discussion

3.1 POLYMER SYNTHESIS AND CHARACTERIZATION

Both poly(acrylic acid) and poly(acrylamide) were synthesized by free radical polymerizations in 1,4-Dioxane using AIBN as an initiator. Table 2 provides the apparent molar masses (determined by size exclusion chromatography) of these polymers. It is clear that inclusion of the individual fluorescent labels ACE and AMMA, with a comparable concentration of initiator, inhibited the polymerization compared to the polymerizations without these comonomers and this results in lower average apparent molar masses. To compensate for the possibility of more substantial retardation when both comonomers were incorporated the dual label polymer was prepared with a much lower concentration of initiator. The polymer produced in this manner was observed to have a much broader, but still symmetrical, distribution than the other PAA polymers. Additionally it was shown, by UV absorbance detection, that both aromatic labels were incorporated across the full molar mass distribution (see supporting information). The presence of small quantities of the hydrophobic labels had no effect on the pKa (pKa 4.5) of the poly(acrylic acid) which was determined via acid-base titration.

Table 2. Apparent molar mass moments (number (M_n), weight (M_w), z average (M_v) and dispersity (Đ) molar mass) of synthesised copolymers* determined by size exclusion chromatography

Polymer	M_n	M_w	M_z	Đ
PAA	58,100	112,550	186,450	1.9
P(AA-*co*-ACE)	42,150	64,900	89,950	1.5
P(AA-*co*-AMMA)	30,050	50,500	72,800	1.6
P(AA-*co*-ACE-*co*-AMMA)	47,100	129,100	229,850	2.7
PAM	9,700	47,900	114,700	4.9
P(AM-*co*-ACE)	2,000	6,400	12,400	3.2
P(AM-*co*-AMMA)	5,000	14,500	20,000	2.9

* Monomer feed of ACE and AMMA less than 1% of copolymer random composition

Dissolved polymer hydrodynamic radius (R_H) and intrinsic viscosity [η] were calculated using diffusion-ordered NMR spectroscopy (DOSY) in D_2O (Table 3). This process uses the proton peak on the ^1H NMR spectra to determine the diffusion (flux) of the polymer in solution, and the proton peak of the solvent to determine solution viscosity. DOSY NMR can provide the size of polymer chains in solution[7, 56] and it is a useful technique to determine the hydrodynamic radii of dissolved polymers[54]. The measurement of the PAA in D_2O provided the radius of PAA at pD = 7.435. DOSY NMR was then used to examine any changes in solution behaviour due to incorporation of the labels. Fig 3 shows R_H measured as the *pH* was changed for the PAA and PAA-*co*-ACE polymers. The data show the familiar expansion of the coil at the pKa and there was no significant differences in the behaviour of the labelled copolymer and the homopolymer.

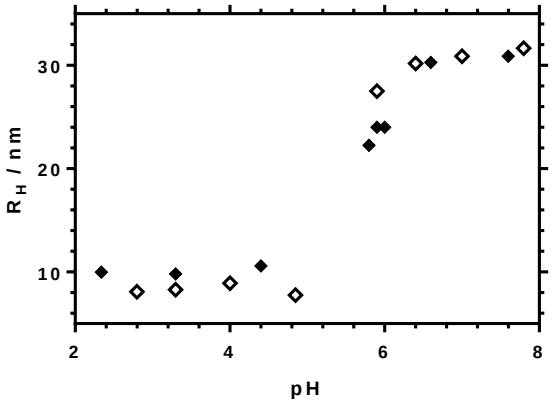

Figure 3. Hydrodynamic radius of PAA (◇) and PAA-co-ACE (◆) in D_2O at varying pH.

As the molar mass of these polymers is known determination of the polymer hydrodynamic radii from diffusion data also yields a measurement of the sample's intrinsic viscosity in aqueous solutions at room temperature[54]. The intrinsic viscosity [η] of these systems appears to increase with molar mass, which is expected. Polymer tacticity was also measured by ^{13}C NMR spectroscopy[30] and the % isotactic (rr and mm) and syndiotactic (mr) calculated from peak integrals (see electronic supporting information for details).

Table 3. Hydrodynamic radii, intrinsic viscosity [η] and polymer tacticity* ratios from NMR measurements

Polymer	% rr	% mr	% mm	R_H / nm	[η] ** / dl g^{-1}
PAA	30.6	50.0	19.4	16.98	0.12
P(AA-*co*-ACE)	14.4	51.1	34.4	9.12	0.03
P(AA-*co*-AMMA)	38.9	50.0	11.1	8.51	0.04
P(AA-*co*-ACE-*co*-AMMA)	43.8	53.1	3.1	17.78	0.12
PAM	34.4	53.1	12.5	9.77	0.06
P(AM-*co*-ACE)	14.6	49.5	35.8	3.98	0.03
P(AM-*co*-AMMA)	7.3	57.3	35.4	8.31	0.11

* Polymer tacticity calculated from ^{13}C NMR integration of peaks 34 – 36 ppm[57]. ** [η] in D_2O, pH 5, at 25 ºC

The ability of these polymers to complex in aqueous conditions was tested by the use of particle sizing via light scattering. PAA binds to poly(acrylamide) via repeated hydrogen bonding to produce suspended aggregated particles, which can be detected via particle sizing techniques[53, 58]. The scattering intensities in dilute acidic solutions of the polymers alone were too weak to provide high quality precise data. However, better quality data were obtained from repeated measurements of the complexes as shown in Figure 4. This shows the particle sizes of the complexed polymers with PAA, P(AA-*co*-ACE) and P(AA-*co*-ACE-*co*-AMMA). Equivalent particle sizes are found for all systems indicating, as previously suggested, that the presence of < 1% of a fluorescent label does not prevent complex formation. These particle sizes were confirmed by adding droplets of complexed particles (0.05 mg ml^{-1} concentration of each component) to a glass microscope slide. Examination of the solution by optical microscopy, at pH 2, revealed small sub-micron particles moving under Brownian motion. When the pH was raised by addition of concentrated NaOH these particles disappeared from view.

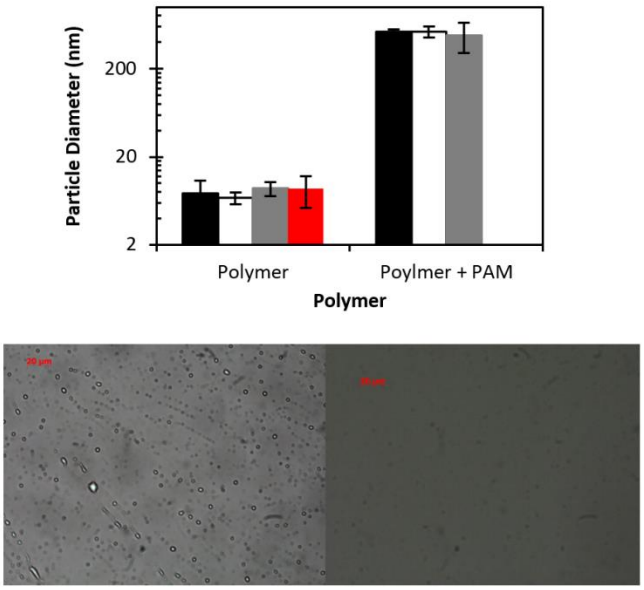

Figure 4. Top: Mean particle diameters of PAA (black), P(AA-co-ACE) (white), P(AA-co-ACE-co-AMMA) (gray) and PAM (red), tested both alone and mixed with equal concentration of PAM. All results tested at pH 2. Bottom: Optical photo-graphs of dilute PAA-PAM mixtures taken at 50x magnification at pH 2 (left) and pH 7 (right).

In summary the dissolved polymers did not scatter sufficient light to give accurate particle sizes but the data indicated that the particle diameters are < 20 nm, in agreement with DOSY NMR data. Although the data from non-complexed polymers was of low quality it was possible after repeated measurements (n = 30) to compare the non-complexed and complexed particle size data using statistical analysis. Thus the complexes were shown to form particles with significantly ($P < 0.01$) larger sizes than the non-complexed. Particle sizing offers independent evidence of IPC formation for use alongside data from fluorescence experiments.

The formation of large (> 200 nm) particles following complex formation indicates that the formation of interpolymer complexes leads to further aggregation. However optical microscopy of these types of materials are subject to significant light scattering, generating coronas around particle diameters, and so are not suitable for measuring particle sizes. Dried samples were then examined by AFM. Comparison of complexed PAA-PAM (Fig. 5A-B) compared to collapsed PAA (Fig. 5C-D) (both at pH 2) show distinct differences after drying. The IPC solution dried forming distinct globular particles that varied in size from 100 – 500 nm whilst the collapsed (but solvated) PAA chains formed a mat, which completely covered the glass slide. Whilst surface features were visible on close inspection of the PAA slide no distinct particles were observed. Further images are provided in the supporting information. The observed discrete particles seen in the complexed samples have similar dimensions to the data provided via DLS measurements showing good agreement between the two analytical techniques.

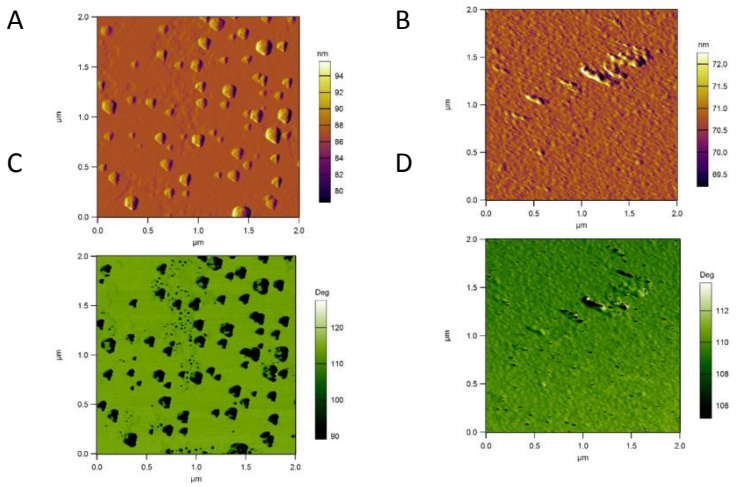

Figure 5. Amplitude (A+C) and phase (B+D) AFM distribution maps of dried PAA-PAM complex (A+B) and PAA (C+D) solutions on a microscope slide.

3.2 ANALYSIS OF FLUORESCENCE LABELS

Fluorescent labels ACE and AMMA both exhibit broad absorption with several distinct peaks. The molar absorption coefficients of derivatives acenaphthene and anthracene in methanol were determined (from 1 to 20 x 10^{-5} mol dm^{-3}) to allow for the loading of the fluorescence label. The absorbance peaks at 290 nm (ACE) and 355 nm (AMMA) were used and their absorption coefficients calculated. It was found that the label functional units exhibited molar absorption coefficients of 5699 M^{-1} cm^{-1} and 7202 M^{-1} cm^{-1} respectively (full data is contained in the supporting information). The peak excitation wavelengths for ACE and AMMA, bound to the polymer, were 295 and 370 nm respectively. The fluorophores exhibited similar properties on and off the polymer backbone, however a larger Stokes shift was observed for the backbone label ACE than the more loosely bound AMMA, a more detailed explanation is discussed in the supporting information. Also, the peak emission wavelengths were 340 and 420 nm. These observations confirmed the well-known overlap of ACE emission and AMMA excitation (Fig. 6), which allows efficient FRET experiments[23, 28]. Dilute solutions of PAA do not excite or emit in these regions and the wavelength of the ACE label does not respond to the pH of the solution (see ESI). The molar absorption coefficients calculated were used to estimate the loading, by weight, of ACE and AMMA onto the polymer backbones. The PAA polymers were shown to have: P(AA-co-ACE) = 1.05 wt% ACE, P(AA-co-AMMA) = 0.32 wt% AMMA, P(AA-co-ACE-co-AMMA) = 0.5 wt% ACE, 0.9 wt% AMMA, P(AM-co-ACE) = 0.45 wt% ACE, P(AM-co-AMMA) = 0.17 wt% AMMA.

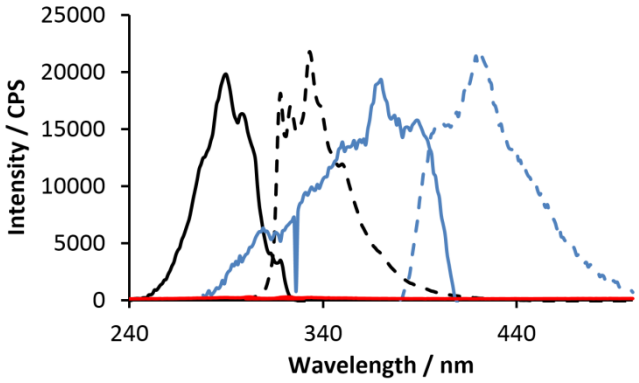

Figure 6. Photoluminescence excitation (solid lines - λ_{exACE}330 nm / λ_{exAMMA}420 nm) & Emission (dashed lines - λ_{emACE}295 nm / λ_{emAMMA}370 nm) spectra of P(AA-*co*-ACE) (black), P(AA-*co*-AMMA) (blue), and PAA (red) aqueous solutions (1 mg ml^{-1}).

As the PAA collapses / swells reversibly with pH, the fluorescence lifetime of the ACE label responds due to the swelling of the polymer coil affecting its ability to shield the fluorophore from the solvent. This does not affect the λem or the Stoke shift of the polymerized label. The fluorescence lifetime can be calculated from the fluorescence decay following excitation. When detached from a polymer the free ACE label studied in dioxane had a lifetime of 11.6 ns (standard deviation 0.04 ns, $\chi^2 = 3$). When attached to a pH sensitive polymer such as PAA the fluorescence lifetime responds to the conformational state of the polymer, so at pH 2 the fluorophore was shielded and decayed over a much longer period compared to the swollen polymer at pH 8 (Fig. 7). The fitted lifetime calculated from these decays show the lifetime shifts between 22 and 35 ns depending on the conformational state of the polymer. Studies using the ACE label on temperature responsive polymers show similar results indicating the deprotonation of the acid group has little effect on the fluorescence lifetime[59].

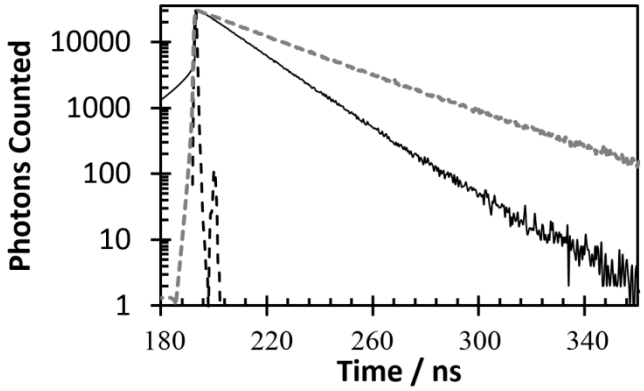

Figure 7. The fluorescence decay of P(AA-co-ACE) with varying pH (pH 8 = black line, pH 2 = dashed grey) with impulse from silica prompt (scattered line) in ns after excitation pulse.

These experiments are only possible in dilute solution, as increasing the polymer concentration raises the concentration of ACE label, which leads to excimer formation[60] and self-quenching of the system. Total quenching (no observed emission at expected wavelengths) of these copolymers occurs above 10 mg ml^{-1}.

Energy transfer measurements on single and dual polymer mixtures were carried out following protocols from Ruiz-Pérez[23], and end to end distances have been calculated assuming a Gaussian distribution can be used to model energy transfer efficiency[29]. Energy transfer measurements that contain both chromophores were measured via both static and dynamic techniques so that the ratio of radiative energy transfer, and non-radiative energy transfer, can be gauged. Static intensity measurements (Figs. 8 – 10) show the total degree of energy transfer in the system, whilst the lifetime measurements (Figs. 13 - 14) report exclusively on non-radiative processes[23]. Combined these provide high detailed short-range information about polymer conformation.

3.3 THE EFFECT OF INTERPOLYMER COMPLEXATION

3.3.1 ENERGY TRANSFER USING EMISSION (E_{ST})

Examining E_{ST} is a standard technique for studying FRET from one chromophore to another. It was employed to study both the proximity of the two polymers (P(AA-co-ACE) and P(AM-*co*-AMMA)) and the state of the PAA component using P(AA-*co*-ACE-*co*-AMMA).

FRET between P(AA-co-ACE) and P(AM-co-AMMA). PAA AMMA was attached to PAM and ACE was attached to the PAA so that FRET would only occur between the two labels if the complex was formed. This experiment allowed us to confirm that complex formation must have occurred and provided evidence that energy transfer occurred across the complexed chains. P(AA-co-ACE) and P(AM-co-AMMA) were mixed at two ratios; 1:1 and 2:1. There was a

broad band emission in the acceptor region (375 – 450 nm) but no distinct peaks from the AMMA (Fig. 8). This result indicates that when the two polymers combine into a single interpolymer complex each label, contained on distinct polymer backbones, are brought together close enough in space to allow FRET to occur across two polymer chains. Using the peak wavelengths from Fig. 6 E_{ST} was calculated to be 0.01, 0.19 and 0.28 as the concentration of PAM increased from 0, 1 and 2 mg ml^{-1} respectively (raw data shown in electronic supporting information).

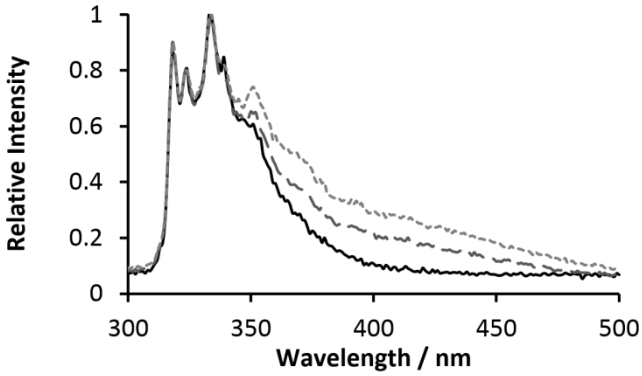

Figure 8. Emission spectra (relative to peak emission at 333nm) of singly labelled polymers P(AA-co-ACE) (solid black line) (1 mg ml-1) with P(AM-co-AMMA) (1 : 1 – dashed line, 1 : 2 – with pH. At low pH dotted line). λex = 295 nm

Doubly labelled PAA The polymer containing both ACE and AMMA can be studied, in the context of energy transfer between the two fluorophores, to show the collapse of the polymer chain[23, 29]. When the polymer is collapsed, and the separation between labels is reduced, there is greater potential for FRET, resulting in quenching of the ACE peak (330 nm) and increased AMMA emission (390 and 410 nm). Steady state measurements were carried out to see the full range of the ACE and AMMA excitations/emissions and the data are shown in Fig. 9. The total energy transfer efficiency across the donor and acceptor labels varied between 15 and 77 % as the pH was adjusted (see supporting information).

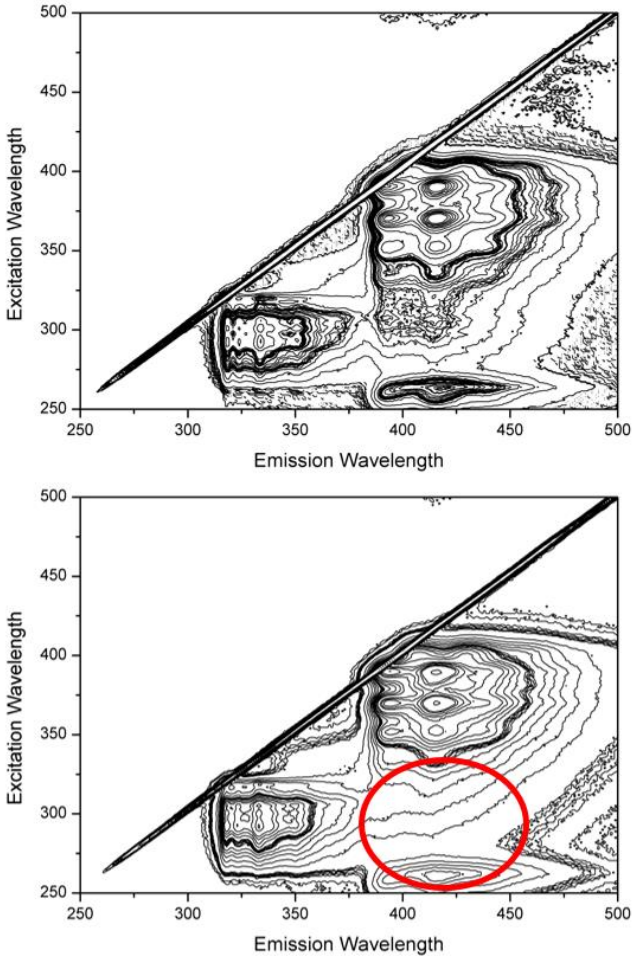

Figure 9. 3D excitation/emission spectrum of P(AA-co-ACE-co-AMMA) at pH 3 (top) and pH 7 (bottom) with contours every half integer from 1 x 10^3 to 2 x 10^5 CPS (counts per second). The red circle denotes energy transfer region of ACE and AMMA.

When an equal concentration of PAM was added to this solution (Fig. 10) there was no change in the spectrum at pH 6 but at pH 3 the ACE peak diminished and there was a slight increase in the AMMA emission.

The data indicated that the amount of energy transfer had increased at pH 3 as the complex was formed. This can only occur if the two labels come into closer contact in the complexed state.

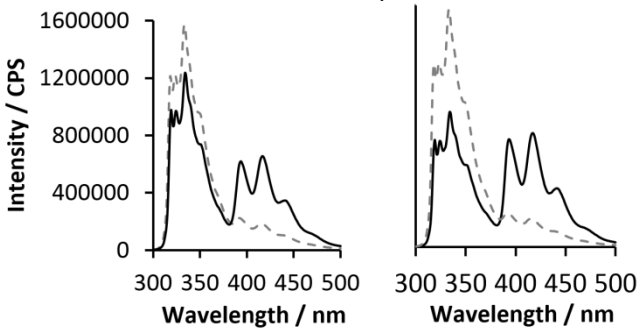

Figure 10. Emission spectra (concentration = 1 mg ml-1) by counts per second. Left: P(AA-co-ACE-co-AMMA), right: P(AA-co-ACE-co-AMMA) mixed with PAM; pH 3 (solid black line) and pH 6 (dashed grey line). λ_{ex} = 295 nm. The data show that energy transfer between the ACE and AMMA labels increases as the complex forms at pH 3.

The amount of static energy transfer (E_{ST}) can be calculated from a comparison of the ACE and AMMA peak height. When the entire spectra of P(AA-*co*-ACE-*co*-AMMA) and 1 : 1 P(AA-*co*-ACE-*co*-AMMA) : PAM in dilute solutions were compared it was seen that energy transfer had increased with interpolymer complexation below pH 3 (Fig. 11). Above pH 3 however the energy transfer between the two labels was comparable between the single and mixed polymer systems.

Considering that the PAA-PAM complex was usually regarded as an extended chain conformational state, this result was unexpected. In the collapsed globular non-complexed state one might expect the PAA chains to bring the ACE and AMMA labels closer together than in the extended ribbon or ladder type structures proposed for the complexed state.

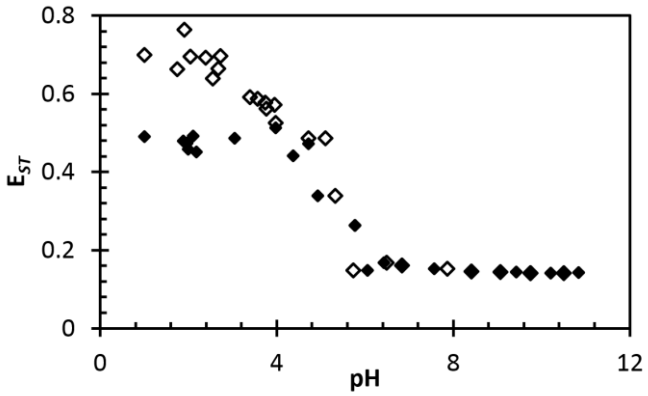

Figure 11. The changing energy transfer of dilute mixtures of P(AA-*co*-ACE-*co*-AMMA) (◇) alone and mixed with an equal concentration of PAM (◆) with pH.

Following on from this result the concentration of P(AA-*co*-ACE-*co*-AMMA) was fixed and the concentration of poly(acrylamide) varied to show that even at very low concentrations of poly(acrylamide) there was an increase in the energy transfer between ACE and AMMA across the polymer backbone (Fig. 12) as PAM was added. The data showed a strong dependence of E_{ST} on concentration of PAM.

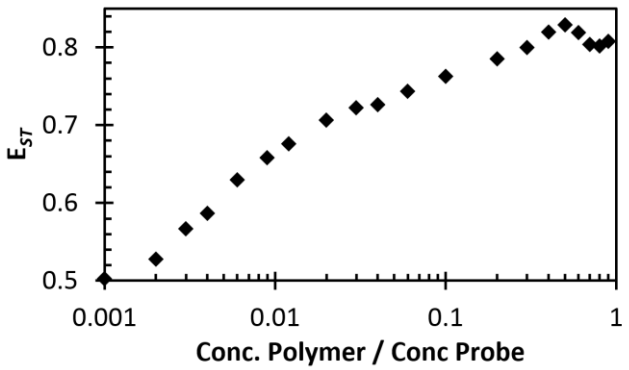

Figure 12. Energy transfer of P(AA-co-ACE-co-AMMA) (1 mg ml^{-1}) with varying PAM concentration at pH 2.

3.3.2 ENERGY TRANSFER USING DYNAMIC TECHNIQUES

Time resolved fluorescence anisotropy has been previously used to detect the interpolymer complexation of poly(acrylic acid) with poly(acrylamide)[15] and with also a range of other polymers[14]. Measurements of $E_{D\tau}$ can be used to study the effect of the acceptor upon the donor. One advantage of this method is in its use for estimating the label separation distance and this was used to study both polymer systems as discussed below.

The life-time of all the labelled PAA systems was dominated by the transition at pH 5 following the deprotonation of the acid backbone. Figure 14 shows how the fluorescence lifetime of the donor changes with pH in P(AA-*co*-ACE). A clear transition was observed at approximately pH 5. Fig 13 shows also similar data derived from P(AA-*co*-ACE-*co*-

AMMA) alone and in the presence of PAM. These data also show a decrease in lifetime, increase in quenching by the medium, below pH 5. However, the data also show that the lifetime of the ACE label in P(AA-co-ACE) is higher below pH 5 than when an acceptor label was added (PAA-co-ACE-co-AMMA). This effect was not observed above pH 5 and indicates energy transfer in the collapsed desolvated state below pH 5 but negligible energy transfer in the solvated coil state (above pH 5). In the presence of PAM there was only a small change in the lifetime. The label separation was estimated to be 2.44 – 2.46 nm for the polymer in the presence of poly(acrylamide) below pH 5, and 2.53 – 2.61 nm in the absence of poly(acrylamide). Therefore the data showed that it was not possible to demonstrate any significant difference in label separation on complexation to poly(acrylamide).

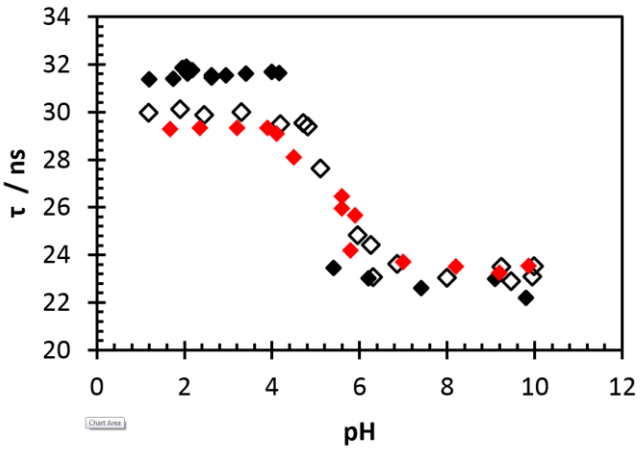

Figure 13. The napthalene fluorescence lifetime (τ) of P(AA-co-ACE) with varying pH (◆), P(AA-co-ACE-co-AMMA) alone (◇) and P(AA-co-ACE-co-AMMA) with PAM (◆). χ^2 of all fluorescence fits are shown in supporting information.

Complexation of P(AA-co-ACE) and P(AM-co-AMMA). When P(AA-co-ACE) and P(AM-co-AMMA) were mixed, FRET was only observable below pH 3 (Fig. 11). Fig. 14 shows that the lifetime of the ACE within P(AA-co-ACE) was not affected by the presence of PAM. However, in the presence of P(AM-co-AMMA), the lifetime of ACE changed at pH 5 with the swelling of the PAA and there was a marked reduction of fluorescence lifetime at pH 3 and below. Therefore this system shows dual transition zones as the label is quenched by the complexing copolymer, then shielded from solvent by the collapsed PAA and then quenched with increasing pH. The data support the hypothesis of polymer-polymer complex formation below pH 3; swelling at pH 3 – 5 followed by solvation induced swelling above pH 5. As the system progressed from pH 3 to 5 the complex swelled and the life time increased as the quenching by AMMA decreased (the labels separated). However, above pH 5 the complex dissociated and the P(AA-*co*-ACE) solvated so that solvent quenching became the dominant process that decreased the lifetime of fluorescence from the ACE label.

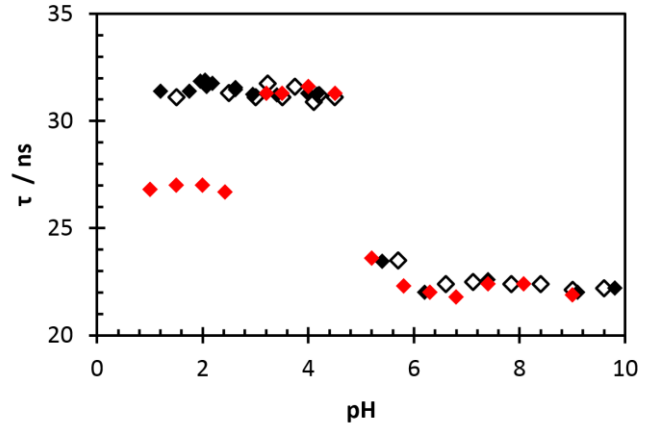

Figure 14. The fluorescence lifetime (τ) of P(AA-co-ACE) with varying pH (◆), in the presence of PAM (◇) and in the presence of P(AM-co-AMMA) (◆).χ^2 of all fluorescence fits are shown in supporting information.

Energy transfer ($E_{D\tau}$) can be calculated from this as 0.15, 0.01 and 0.04 when the PAA is complexed, swollen and solvated respectively. Label separation calculations showed that in the complex form the fluorescence labels were on average 2.46 nm apart, a smaller separation than observed for any of the dual labelled systems.

4. Discussion

Complexes of PAA bound to PAM have been widely reported but few studies of the conformations of the polymers in the complexed or isolated state have been carried out. Complex formation by hydrogen bonding between PAA and PAM was confirmed using light scattering and AFM. AFM measurements of the complexes showed that they formed almost spherical structures rather than being fibrillar. FRET was then used to study the nature of these complexes. PAA containing both a donor and an acceptor label was complexed with PAM. Upon mixing of these two polymers the amount of energy transfer between the two labels increased. This was result was not expected because the data indicated that the PAA chains become more compact upon binding and this is not consistent with the formation of a complex composed of extended chains as implied in the "zipper". However, the result is consistent with the hypothesis put forward by Deng et al.[53] In their work it is proposed that the fractions of the chains exist as aggregates, prior to complexation, rather than isolated chains. Then the complex is thought to evolve within these aggregates. The data can be explained by considering the formation of the interpolymer complex as a desolvation transition to a co-globular structure with the inter-label distance decreasing on complexation because the swelling of the PAA decreases on desolvation/complex formation. In this model the complex formation provides a further desolvation process as hydrogen bonds to PAM form.

Experiments with the labels on separate polymers (PAA-*co*-ACE) and P(AM-*co*-AMMA) provided evidence (Table 4) for a dual transition in the PAA between complexed, collapsed and swollen structures. In a model that is consistent with these data (Fig 15) a tight desolvated co-globular structure would be formed at pH < 3. In this structure quenching would have occurred between the two labels on the different polymers because they were held in close proximity. Then as the pH increased the P(AA-*co*-ACE) swelled and the labels became more distant so that the quenching effect of the AMMA decreased. However, the swelling process did not expose the label to the quenching effects of the solvent until at > pH 5 the P(AA-*co*-ACE) became solvated and the complex fully dissociated.

In the P(AA-*co*-ACE-*co*-AMMA) system Förster energy transfer increased on complexation and this indicated that the PAA became desolvated to a greater extent when complexed to PAM. These new results indicated that the PAA segments are in close proximity in the PAA-PAM complex, circa 2-3 nm.

Table 4. Summary of Energy Transfer Results*

Sample		< pH 3	pH 3 - 5	> pH 5
P(AA-*co*-ACE) with P(AM-*co*-AMMA)				
	r / nm	2.16	>5	>5
	E_{ST}	0.19	0.00	0.00
P(AA-*co*-ACE-*co*-AMMA) alone				
	r / nm	2.61	2.53	>5
	E_{ST}	0.50	0.50	0.17
P(AA-*co*-ACE-*co*-AMMA) with PAM				
	r / nm	2.46	2.44	>5
	E_{ST}	0.71	0.51	0.17

* Horizontal lines drawn to show where techniques detect clear state change in material.

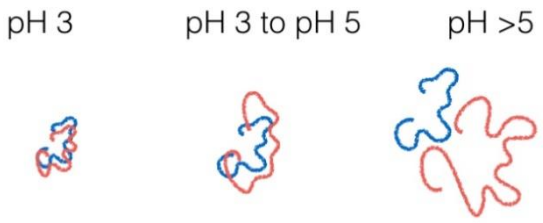

Figure 15. Dual polymer system shows two transitions; at pH 3 and at pH 5 reflecting three states of poly(acrylic acid) (complexed, dissociated and swollen).

5. Conclusions

At low pH the protonated Poly(acrylic acid) forms an interpolymer complex with poly(acrylamide) in the form coglobule without chain extension. Between pH 3 to 5 the globular complex appears to be increasingly swollen and then at pH > 5 the complex dissociates into solvated separate chains.

6. Additional Information

Author Information

[a] *Polymer laboratories, School of Chemistry and Bioscience, Richmond Road, University of Bradford, Bradford, South Yorkshire, BD7 1DP, UK.*
[b] *Polymer and Biomaterials Chemistry Laboratories, Department of Chemistry, Brook Hill, University of Sheffield, Sheffield, South Yorkshire, S3 7HD, UK.*
† Electronic Supplementary Information (ESI) available: additional details and data of polymer characterization, diffusion NMR, ^{13}C NMR, Jablonski diagrams, molar absorption coefficients, ACE/AMMA label response to pH, pKa calculations, Stokes Shift analysis, Label Molar Mass Distribution, Turbidity of Solution, Particle Size by DLS, Fluorescence Lifetimes Fitting, $E_{D\tau}$ of all systems, E_{ST} of all systems, Optical Microscopy, AFM Microscopy, additional references. Raw data]. See DOI: 10.1039/x0xx00000x

Acknowledgements

Thanks to Stephen Hickey of the University of Bradford for advice on fluorescence analytical methodology during the preparation of this manuscript. This work was carried out in part thanks to an EPSRC CASE funded PhD studentship at the University of Sheffield, sponsored by SNF (UK) Ltd.

Notes and references

‡ Address correspondence to Dr Thomas Swift and Professor Stephen Rimmer, University of Bradford, Great Horton Road, BD7 1DP. Emails t.swift@bradford.ac.uk, s.rimmer@bradford.ac.uk. Phone +44 (0) 1274 236231.

1. Chen, S.; Fahmi, N. E.; Wang, L.; Bhattacharya, C.; Benkovic, S. J.; Hecht, S. M., Detection of Dihydrofolate Reductase Conformational Change by FRET Using Two Fluorescent Amino Acids. *Journal of the American Chemical Society* **2013,** *135* (35), 12924-12927.
2. Watkins, H. M.; Simon, A. J.; Sosnick, T. R.; Lipman, E. A.; Hjelm, R. P.; Plaxco, K. W., Random coil negative control reproduces the discrepancy between scattering and FRET measurements of denatured protein dimensions. *Proceedings of the National Academy of Sciences* **2015,** *112* (21), 6631-6636.
3. Cattoz, B.; de Vos, W. M.; Cosgrove, T.; Crossman, M.; Espidel, Y.; Prescott, S. W., Interpolymer Complexation: Comparisons of Bulk and Interfacial Structures. *Langmuir* **2015,** *31* (14), 4151-4159.
4. Baranovsky, V. Y.; Litmanovich, A. A.; Papisov, I. M.; Kabanov, V. A., Quantitative studies of interaction between complementary polymers and oligomers in solutions. *European Polymer Journal* **1981,** *17* (9), 969-979.
5. Ilmain, F.; Tanaka, T.; Kokufuta, E., Volume transition in a gel driven by hydrogen bonding. *Nature* **1991,** *349* (6308), 400-401.
6. Teresa Garay, M.; Cristina Llamas, M.; Iglesias, E., Study of polymer-polymer complexes and blends of poly(N-isopropylacrylamide) with poly(carboxylic acid): 1. Poly(acrylic acid) and poly(methacrylic acid). *Polymer* **1997,** *38* (20), 5091-5096.
7. Winnik, M. A.; Yekta, A., Associative polymers in aqueous solution. *Current Opinion in Colloid & Interface Science* **1997,** *2* (4), 424-436.
8. Slager, J.; Domb, A. J., Biopolymer stereocomplexes. *Advanced Drug Delivery Reviews* **2003,** *55* (4), 549-583.

9. Staikos, G.; Bokias, G.; Tsitsilianis, C., The viscometric methods in the investigation of the polyacid-polybase interpolymer complexes. *Journal of Applied Polymer Science* **1993,** *48* (2), 215-217.
10. Yan, X.; Li, S.; Pollock, J. B.; Cook, T. R.; Chen, J.; Zhang, Y.; Ji, X.; Yu, Y.; Huang, F.; Stang, P. J., Supramolecular polymers with tunable topologies via hierarchical coordination-driven self-assembly and hydrogen bonding interfaces. *Proceedings of the National Academy of Sciences* **2013,** *110* (39), 15585-15590.
11. Das, S.; Joseph, M. T.; Sarkar, D., Hydrogen Bonding Interpolymer Complex Formation and Study of Its Host–Guest Interaction with Cyclodextrin and Its Application as an Active Delivery Vehicle. *Langmuir* **2013,** *29* (6), 1818-1830.
12. Endo, N.; Shirota, H.; Horie, K., Deuterium Isotope Effect on the Phase Separation of Zipper-Type Hydrogen-Bonding Inter-Polymer Complexes in Solution. *Macromolecular Rapid Communications* **2001,** *22* (8), 593-597.
13. Lee, H.; Mensire, R.; Cohen, R. E.; Rubner, M. F., Strategies for Hydrogen Bonding Based Layer-by-Layer Assembly of Poly(vinyl alcohol) with Weak Polyacids. *Macromolecules* **2012,** *45* (1), 347-355.
14. Swift, T.; Swanson, L.; Bretherick, A.; Rimmer, S., Measuring poly(acrylamide) flocculants in fresh water using inter-polymer complex formation. *Environmental Science: Water Research & Technology* **2015,** *1* (3), 332-340.
15. Swift, T.; Swanson, L.; Rimmer, S., Poly(acrylic acid) interpolymer complexation: use of a fluorescence time resolved anisotropy as a poly(acrylamide) probe. *RSC Advances* **2014,** *4* (101), 57991-57995.
16. Thapaliya, E. R.; Fowley, C.; Callan, B.; Tang, S.; Zhang, Y.; Callan, J. F.; Raymo, F. M., Energy-Transfer Schemes To Probe Fluorescent Nanocarriers and Their Emissive Cargo. *Langmuir* **2015,** *31* (35), 9557-9565.
17. Moharram, M. A.; Soliman, M. A.; El-Gendy, H. M., Electrical conductivity of poly(acrylic acid)–polyacrylamide complexes. *Journal of Applied Polymer Science* **1998,** *68* (12), 2049-2055.
18. Garces, F. O.; Sivadasan, K.; Somasundaran, P.; Turro, N. J., Interpolymer complexation of poly(acrylic acid) and polyacrylamide: structural and dynamic studies by solution- and solid-state NMR. *Macromolecules* **1994,** *27* (1), 272-278.
19. Sivadasan, K.; Somasundaran, P.; Turro, N. J., Fluorescence and viscometry study of complexation of poly(acrylic acid) with poly(acrylamide) and hydrolysed poly(acrylamide). *Colloid and Polymer Science* **1991,** *269* (2), 131-137.
20. Sivadasan, K.; Somasundaran, P., Complexation of hydrolyzed poly(acrylamide) with poly(acrylic acid) by excimer fluorescence measurements of pyrene labeled polymers. *Journal of Polymer Science Part A: Polymer Chemistry* **1991,** *29* (6), 911-914.
21. Bian, F.; Liu, M., Complexation between poly(N,N-diethylacrylamide) and poly(acrylic acid) in aqueous solution. *European Polymer Journal* **2003,** *39* (9), 1867-1874.
22. Plenderleith, R.; Swift, T.; Rimmer, S., Highly-branched poly(N-isopropyl acrylamide)s with core-shell morphology below the lower critical solution temperature. *RSC Advances* **2014,** *4* (92), 50932-50937.
23. Ruiz-Pérez, L.; Pryke, A.; Sommer, M.; Battaglia, G.; Soutar, I.; Swanson, L.; Geoghegan, M., Conformation of Poly(methacrylic acid) Chains in Dilute Aqueous Solution. *Macromolecules* **2008,** *41* (6), 2203-2211.
24. Pietsch, C.; Schubert, U. S.; Hoogenboom, R., Aqueous polymeric sensors based on temperature-induced polymer phase transitions and solvatochromic dyes. *Chemical Communications* **2011,** *47* (31), 8750-8765.
25. Haley, J. C.; Liu, Y.; Winnik, M. A.; Demmer, D.; Haslett, T.; Lau, W., Tracking polymer diffusion in a wet latex film with fluorescence resonance energy transfer. *Review of Scientific Instruments* **2007,** *78* (8), 084101.
26. Sparks, D. J.; Romero-Gonzalez, M. E.; El-Taboni, E.; Freeman, C. L.; Hall, S. A.; Kakonyi, G.; Swanson, L.; Banwart, S. A.; Harding, J. H., Adsorption of poly acrylic acid onto the surface of calcite: an experimental and simulation study. *Physical Chemistry Chemical Physics* **2015,** *17* (41), 27357-27365.
27. Swift, T.; Swanson, L.; Geoghegan, M.; Rimmer, S., The pH-responsive behaviour of poly(acrylic acid) in aqueous solution is dependent on molar mass. *Soft Matter* **2016,** *12* (9), 2542-2549.
28. Swift, T.; Lapworth, J.; Swindells, K.; Swanson, L.; Rimmer, S., pH responsive highly branched poly(N-isopropylacrylamide) with trihistidine or acid chain ends. *RSC Advances* **2016,** *6* (75), 71345-71350.
29. Liu, G.; Guillet, J.; Al-Takrity, E. T. B.; Jenkins, A.; Walton, D., Dimensions of polyelectrolytes using the" spectroscopic ruler". 2. Conformational changes of poly (methacrylic acid) chains with variation in pH. *Macromolecules* **1991,** *24* (1), 68-74.
30. Barone, G.; Crescenzi, V.; Liquori, A. M.; Quadrifoglio, F., Solubilization of polycyclic aromatic hydrocarbons in poly(methacrylic acid) aqueous solutions. *The Journal of Physical Chemistry* **1967,** *71* (7), 2341-2345.
31. Hargreaves, J. S.; Webber, S. E., Photophysics of anthracene polymers: fluorescence, singlet energy migration, and photodegradation. *Macromolecules* **1984,** *17* (2), 235-240.
32. Gacal, B.; Durmaz, H.; Tasdelen, M. A.; Hizal, G.; Tunca, U.; Yagci, Y.; Demirel, A. L., Anthracene−Maleimide-Based Diels−Alder “Click Chemistry” as a Novel Route to Graft Copolymers. *Macromolecules* **2006,** *39* (16), 5330-5336.
33. Holden, D. A.; Guillet, J. E., Singlet Electronic Energy Transfer in Polymers Containing Naphthalene and Anthracene Chromophores. *Macromolecules* **1980,** *13* (2), 289-295.
34. Deniz, A. A.; Dahan, M.; Grunwell, J. R.; Ha, T.; Faulhaber, A. E.; Chemla, D. S.; Weiss, S.; Schultz, P. G., Single-pair fluorescence resonance energy transfer on freely diffusing molecules: Observation of Förster distance dependence and subpopulations. *Proceedings of the National Academy of Sciences* **1999,** *96* (7), 3670-3675.
35. Wu, P. G.; Brand, L., Resonance Energy Transfer: Methods and Applications. *Analytical Biochemistry* **1994,** *218* (1), 1-13.
36. Wang, S.; Gaylord, B. S.; Bazan, G. C., Fluorescein Provides a Resonance Gate for FRET from Conjugated Polymers to DNA Intercalated Dyes. *Journal of the American Chemical Society* **2004,** *126* (17), 5446-5451.
37. Gaylord, B. S.; Heeger, A. J.; Bazan, G. C., DNA detection using water-soluble conjugated polymers and peptide nucleic acid probes. *Proceedings of the National Academy of Sciences* **2002,** *99* (17), 10954-10957.
38. Tang, Y.; Feng, F.; Yu, M.; An, L.; He, F.; Wang, S.; Li, Y.; Zhu, D.; Bazan, G. C., Direct Visualization of Glucose Phosphorylation with a Cationic Polythiophene. *Advanced Materials* **2008,** *20* (4), 703-705.

39. Wang, C.; Tang, Y.; Liu, Y.; Guo, Y., Water-Soluble Conjugated Polymer as a Platform for Adenosine Deaminase Sensing Based on Fluorescence Resonance Energy Transfer Technique. *Analytical Chemistry* **2014,** *86* (13), 6433-6438.
40. Feng, L.; Zhu, C.; Yuan, H.; Liu, L.; Lv, F.; Wang, S., Conjugated polymer nanoparticles: preparation, properties, functionalization and biological applications. *Chemical Society Reviews* **2013,** *42* (16), 6620-6633.
41. Zhang, J.; Xing, B.; Song, J.; Zhang, F.; Nie, C.; Jiao, L.; Liu, L.; Lv, F.; Wang, S., Associated Analysis of DNA Methylation for Cancer Detection Using CCP-Based FRET Technique. *Analytical Chemistry* **2014,** *86* (1), 346-350.
42. Feng, X.; Liu, L.; Wang, S.; Zhu, D., Water-soluble fluorescent conjugated polymers and their interactions with biomacromolecules for sensitive biosensors. *Chemical Society Reviews* **2010,** *39* (7), 2411-2419.
43. Song, J.; Zhang, J.; Lv, F.; Cheng, Y.; Wang, B.; Feng, L.; Liu, L.; Wang, S., Multiplex Detection of DNA Mutations by the Fluorescence Fingerprint Spectrum Technique. *Angewandte Chemie* **2013,** *125* (49), 13258-13261.
44. Liu, B.; Gaylord, B. S.; Wang, S.; Bazan, G. C., Effect of Chromophore-Charge Distance on the Energy Transfer Properties of Water-Soluble Conjugated Oligomers. *Journal of the American Chemical Society* **2003,** *125* (22), 6705-6714.
45. Peng, K.-Y.; Chen, S.-A.; Fann, W.-S., Efficient Light Harvesting by Sequential Energy Transfer across Aggregates in Polymers of Finite Conjugational Segments with Short Aliphatic Linkages. *Journal of the American Chemical Society* **2001,** *123* (46), 11388-11397.
46. Chee, C. K.; Rimmer, S.; Soutar, I.; Swanson, L., Time-resolved fluorescence anisotropy studies of the interaction of N-isopropyl acrylamide based polymers with sodium dodecyl sulphate. *Soft Matter* **2011,** *7* (10), 4705-4714.
47. Inal, S.; Kölsch, J. D.; Chiappisi, L.; Kraft, M.; Gutacker, A.; Janietz, D.; Scherf, U.; Gradzielski, M.; Laschewsky, A.; Neher, D., Temperature-Regulated Fluorescence Characteristics of Supramolecular Assemblies Formed By a Smart Polymer and a Conjugated Polyelectrolyte. *Macromolecular Chemistry and Physics* **2013,** *214* (4), 435-445.
48. Cerdan, L.; Enciso, E.; Gartzia-Rivero, L.; Banuelos, J.; Arbeloa, I. L.; Costela, A.; Garcia-Moreno, I., A FRET analysis of dye diffusion in core/shell polymer nanoparticles. *RSC Advances* **2014,** *4* (42), 22115-22122.
49. Sarker, P.; Swindells, K.; Douglas, C. W. I.; MacNeil, S.; Rimmer, S.; Swanson, L., Forster resonance energy transfer confirms the bacterial-induced conformational transition in highly-branched poly(N-isopropyl acrylamide with vancomycin end groups on binding to Staphylococcus aureus. *Soft Matter* **2014,** *10* (31), 5824-5835.
50. Giusti, F.; Popot, J.-L.; Tribet, C., Well-Defined Critical Association Concentration and Rapid Adsorption at the Air/Water Interface of a Short Amphiphilic Polymer, Amphipol A8-35: A Study by Förster Resonance Energy Transfer and Dynamic Surface Tension Measurements. *Langmuir* **2012,** *28* (28), 10372-10380.
51. Bassam, B. J.; Caetano-Anollés, G., Silver staining of DNA in polyacrylamide gels. *Applied Biochemistry and Biotechnology* **1993,** *42* (2), 181-188.
52. Nawaz, M. A.; Aman, A.; Rehman, H. U.; Bibi, Z.; Ansari, A.; Islam, Z.; Khan, I. A.; Qader, S. A. U., Polyacrylamide Gel-Entrapped Maltase: An Excellent Design of Using Maltase in Continuous Industrial Processes. *Applied Biochemistry and Biotechnology* **2016,** *179* (3), 383-397.
53. Deng, L.; Wang, C.; Li, Z.-C.; Liang, D., Re-examination of the "Zipper Effect" in Hydrogen-Bonding Complexes. *Macromolecules* **2010,** *43* (6), 3004-3010.
54. Swift, T.; Hoskins, R.; Telford, R.; Plenderleith, R.; Pownall, D.; Rimmer, S., Analysis Using Size Exclusion Chromatography of poly(N-isopropyl acrylamide) using Methanol as an Eluent. *Journal of Chromatography A*.
55. Bravo, J.; Mendicuti, F.; Saiz, E.; Mattice, W. L., The Förster radius for energy transfer from naphthalene to anthracene in polyesters with oxyethylene spacers. *Macromolecular Chemistry and Physics* **1996,** *197* (4), 1349-1360.
56. Newkome, G. R.; Young, J. K.; Baker, G. R.; Potter, R. L.; Audoly, L.; Cooper, D.; Weis, C. D.; Morris, K.; Johnson Jr, C. S., Cascade polymers. 35. pH dependence of hydrodynamic radii of acid-terminated dendrimers. *Macromolecules* **1993,** *26* (9), 2394-2396.
57. Chang, C.; Muccio, D. D.; St. Pierre, T., Determination of the tacticity and analysis of the pH titration of poly(acrylic acid) by proton and carbon-13 NMR. *Macromolecules* **1985,** *18* (11), 2154-2157.
58. Khutoryanskaya, O. V.; Morrison, P. W. J.; Seilkhanov, S. K.; Mussin, M. N.; Ozhmukhametova, E. K.; Rakhypbekov, T. K.; Khutoryanskiy, V. V., Hydrogen-Bonded Complexes and Blends of Poly(acrylic acid) and Methylcellulose: Nanoparticles and Mucoadhesive Films for Ocular Delivery of Riboflavin. *Macromolecular Bioscience* **2014,** *14* (2), 225-234.
59. Chee, C. K.; Rimmer, S.; Soutar, I.; Swanson, L., Fluorescence investigations of the thermally induced conformational transition of poly(N-isopropylacrylamide). *Polymer* **2001,** *42* (12), 5079-5087.
60. Reid, R. F.; Soutar, I., Intramolecular excimer formation in macromolecules. II. Energy migration and excimer formation in acenaphthylene-methyl methacrylate copolymers. *Journal of Polymer Science: Polymer Physics Edition* **1980,** *18* (3), 457-467.